Transient External 3D Excitation of a Dispersive and Antisotropic Slab

Friden, Jonas; Kristensson, Gerhard

1995

CODEN:LUTEDX/(TEAT-7043)/1-25/(1995)

Transient External 3D Excitation of a Dispersive and Anisotropic Slab

Jonas Fridén and Gerhard Kristensson

Department of Electroscience
Electromagnetic Theory
Lund Institute of Technology
Sweden

Jonas Fridén

Institute of Theoretical Physics
Chalmers University of Technology
University of Göteborg
SE-412 96 Göteborg
Sweden

Gerhard Kristensson

Department of Electromagnetic Theory
Lund Institute of Technology
P.O. Box 118
SE-221 00 Lund
Sweden

Editor: Gerhard Kristensson

Abstract

Propagation of a transient electromagnetic field in a stratified, dispersive and anisotropic slab and related direct and inverse problems are investigated. The field is generated by a transient external 3D source. The analysis relies on the wave splitting concept and a two-dimensional Fourier transformation in the transverse spatial coordinates. An investigation of the physical properties of the split fields is made. To solve the direct and inverse scattering problems, wave propagators are used. This method is a generalization and a unification of the previously used imbedding and Green functions methods. The wave propagator approach provides an exact solution of the transmission operator. From this solution it is possible to extract the first precursor (the Sommerfeld forerunner). These results also hold for a bi-anisotropic slab. An inverse problem is outlined using reflection and transmission data corresponding to four, two-dimensional Fourier parameters. Due to the stratification of the medium, the inverse Fourier transformation is not needed in the inverse problem.

1 Introduction

Electromagnetic wave propagation is traditionally treated using fixed frequency methods. In recent years, however, the use of time domain techniques has increased. This is due to both new technical development in, e.g. fast computers and generators of short pulses, as well as new theoretical and mathematical approaches.

The inverse scattering problem of retrieving the parameters of the medium from scattering data has an attractive formulation in the time domain [1, 2, 4, 8, 10–13, 15, 16, 19–21, 24, 28, 31–37, 39, 41, 44, 46]. Recently, there has also been advances in the mathematical formulation of the first precursor (the Sommerfeld forerunner) problem in dispersive and inhomogeneous media [45].

The time domain analysis, as it is presented in this paper, relies on the concept of wave splitting, see Refs 8, 9. Crudely speaking, the wave splitting is a decomposition of the fields with respect to the position of their sources [47–51]. The one-dimensional wave splitting technique has been employed for normally or obliquely incident plane waves and a wide class of media, both spatially inhomogeneous, non-dispersive media [8, 19–21, 31–34, 39, 46] and temporally dispersive, homogeneous media [4, 13, 15, 16, 35–37, 41, 44].

In higher dimensions the concept of wave splitting has been developed [47–51]. Moreover, propagation of transient electromagnetic waves in a waveguide with arbitrary cross section has been addressed with wave splitting techniques and in this case the Klein-Gordon equation is decomposed, see Ref. 30.

This paper is a continuation of previous work for anisotropic media [13, 15, 16]. The major objective is to further develop tools to solve the inverse scattering problem. The inverse scattering problem can be solved using several plane waves [15]. In this paper these results are generalized in that the incident field is arbitrary and not necessarily restricted to plane waves. This is accomplished by a Fourier transformation over the two coordinates transverse to the stratification of the medium. The inverse scattering problem can then be solved using the fields for a discrete set

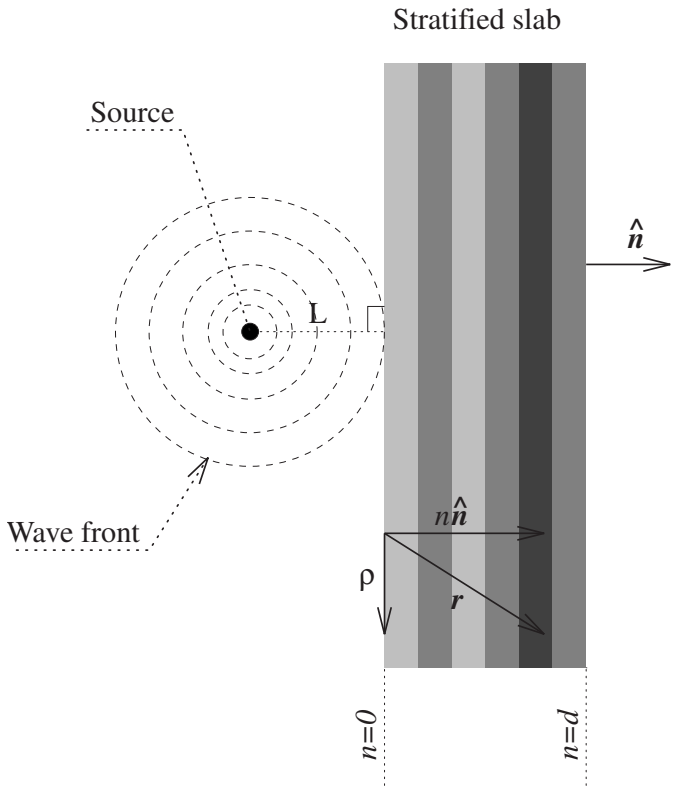

Figure 1: The geometry of the problem at $\tau = 0$ and the source located at $n = -L$.

of Fourier parameters, see also Ref. 20 for a similar treatment for isotropic media. These fields correspond to only one single excitation of the slab with sources on one side of the slab only. This is so due to the fact that the anisotropic medium is invariant under spatial reversion [38, 40]. For a more general bi-anisotropic medium, the same method applies slightly extended using sources on both sides of the slab. Note that the solution of the inverse problem does not require any inverse Fourier transformation of the data and the method is non-iterative.

2 Prerequisites

The transient electromagnetic pulse is generated by a three-dimensional source located outside the slab. The slab is assumed to consist of a general, dispersive, anisotropic medium, which is inhomogeneous with respect to depth, see Figure 1. Outside the slab the medium is assumed to be vacuum. Hence, the parameters of the medium vary only with time and depth, due to the temporal dispersion and the stratification, respectively. Furthermore, no optical response is assumed in the medium. This implies that the wave front velocity, $c_0 = (\epsilon_0 \mu_0)^{-1/2}$, is constant everywhere.

The analysis is based on the Maxwell equations in a source-free region

$$\begin{cases} \nabla \times \boldsymbol{E} = -c_0 \partial_\tau \boldsymbol{B}, \\ \nabla \times \boldsymbol{H} = c_0 \partial_\tau \boldsymbol{D}, \end{cases}$$

where the time unit $\tau = c_0 t$ is used. The constitutive relations used in this paper are

$$\begin{cases} \boldsymbol{D} = \epsilon_0 (\boldsymbol{E} + \boldsymbol{\chi}_e * \boldsymbol{E}), \\ \boldsymbol{B} = \mu_0 (\boldsymbol{H} + \boldsymbol{\chi}_m * \boldsymbol{H}). \end{cases}$$

The permittivity and the permeability of vacuum are denoted ϵ_0 and μ_0, respectively. The symbol $*$ denotes causal, temporal convolution, and an underlying scalar product for convolution of dyadics $\mathbf{A}$ or vectors $\boldsymbol{f}$, i.e.,

$$\mathbf{A}(\tau) * \boldsymbol{f}(\tau) = \int_{-\infty}^{\tau} \mathbf{A}(\tau - \tau') \cdot \boldsymbol{f}(\tau') \mathrm{d}\tau'.$$

In this paper all vectors are typed in italic boldface and all dyadics are typed in Roman boldface or Greek boldface.

Furthermore, let the fields $\boldsymbol{E}((\boldsymbol{r}, t))$ and $\boldsymbol{H}((\boldsymbol{r}, t))$ be quiescent before $\tau < -L$ where L is the distance between the slab and the source. Hence, by causality, the fields in the slab are identically zero for $\tau < 0$. The situation at $\tau = 0$ is depicted in Figure 1.

The constitutive relations model the anisotropic dispersion of the medium [26]. These dispersion effects are represented by the three-dimensional susceptibility dyadics $\boldsymbol{\chi}_\kappa$ with indices $\kappa = e, m$ for electric or magnetic susceptibility, respectively. Due to causality, the susceptibility dyadics $\boldsymbol{\chi}_e(n, \tau)$ and $\boldsymbol{\chi}_m(n, \tau)$ vanish when $\tau < 0$. Outside the slab the susceptibility dyadics vanish for all time τ, since the medium there is vacuum.

Elimination of the fields $\boldsymbol{B}$ and $\boldsymbol{D}$ leads to

$$\begin{cases} \nabla \times \boldsymbol{E}((\boldsymbol{r}, t)) = -\partial_\tau (\eta_0 \boldsymbol{H} + \boldsymbol{\chi}_m * \eta_0 \boldsymbol{H})((\boldsymbol{r}, t)), \\ \nabla \times \eta_0 \boldsymbol{H}((\boldsymbol{r}, t)) = \partial_\tau (\boldsymbol{E} + \boldsymbol{\chi}_e * \boldsymbol{E})((\boldsymbol{r}, t)). \end{cases} \tag{2.1}$$

where the wave impedance of vacuum is denoted $\eta_0 = (\mu_0/\epsilon_0)^{1/2}$.

The spatial variable $\boldsymbol{r}$ is decomposed in a normal and a parallel component with respect to the slab. Explicitly, let $\hat{\boldsymbol{n}}$ be the constant unit vector normal to the interface of the slab and decompose

$$\boldsymbol{r} = \boldsymbol{\rho} + n\hat{\boldsymbol{n}},$$

where $\boldsymbol{\rho} \cdot \hat{\boldsymbol{n}} = 0$. Hence, the coordinate n measures depth, and in the slab $n \in [0, d]$, see also Figure 1.

3 Conversion of the Maxwell equations

The objective of this section is to convert the Maxwell equations into a system of first order equations in the electromagnetic fields parallel to the interfaces of the slab.

The first step in this procedure is to apply a two-dimensional Fourier transform perpendicular to $\hat{\boldsymbol{n}}$. Define $\boldsymbol{\lambda}\cdot\hat{\boldsymbol{n}}=0$ and $|\boldsymbol{\lambda}|=\lambda$. Recall, due to the stratification of the medium, $\boldsymbol{\chi}_e(\boldsymbol{r},\tau)=\boldsymbol{\chi}_e(n,\tau)$ and $\boldsymbol{\chi}_m(\boldsymbol{r},\tau)=\boldsymbol{\chi}_m(n,\tau)$.

Define the two-dimensional Fourier-transform and the inverse transform.

$$\begin{cases} \boldsymbol{H}(\boldsymbol{\lambda},n,\tau)=\displaystyle\iint_{\mathbb{R}^2}\boldsymbol{H}(\boldsymbol{\rho},n,\tau)e^{i\boldsymbol{\lambda}\cdot\boldsymbol{\rho}}d\boldsymbol{\rho}, \\ \boldsymbol{H}(\boldsymbol{\rho},n,\tau)=\dfrac{1}{4\pi^2}\displaystyle\iint_{\mathbb{R}^2}\boldsymbol{H}(\boldsymbol{\lambda},n,\tau)e^{-i\boldsymbol{\lambda}\cdot\boldsymbol{\rho}}d\boldsymbol{\lambda}. \end{cases} \tag{3.1}$$

Note that the nabla operator $\nabla\to-i\boldsymbol{\lambda}+\hat{\boldsymbol{n}}\partial_n$. In the following, the Fourier parameter $\boldsymbol{\lambda}$ is suppressed, e.g. $\boldsymbol{F}(\boldsymbol{\lambda},n,\tau)=\boldsymbol{F}(n,\tau)$.

Decompose the fields and the dyadics in the normal and parallel components with respect to the slab.

$$\begin{cases} \boldsymbol{H}=\boldsymbol{H}_\parallel+H_n\hat{\boldsymbol{n}},\quad \boldsymbol{E}=\boldsymbol{E}_\parallel+E_n\hat{\boldsymbol{n}}, \\ \boldsymbol{\chi}_\kappa=\boldsymbol{\chi}_{\parallel,\kappa}+\hat{\boldsymbol{n}}\boldsymbol{a}_\kappa+\boldsymbol{b}_\kappa\hat{\boldsymbol{n}}+\hat{\boldsymbol{n}}c_\kappa\hat{\boldsymbol{n}},\quad \kappa=e,m, \\ \mathbf{I}=\mathbf{I}_\parallel+\hat{\boldsymbol{n}}\hat{\boldsymbol{n}}. \end{cases}$$

Here the vectors $\boldsymbol{H}_\parallel$, $\boldsymbol{E}_\parallel$, $\boldsymbol{a}_\kappa$, $\boldsymbol{b}_\kappa$ and the dyadics $\boldsymbol{\chi}_{\parallel,\kappa}$ are two-dimensional in the plane normal to $\hat{\boldsymbol{n}}$, e.g. $\hat{\boldsymbol{n}}\cdot\boldsymbol{H}_\parallel=0$, and $\hat{\boldsymbol{n}}\cdot\boldsymbol{\chi}_{\parallel,\kappa}=\boldsymbol{\chi}_{\parallel,\kappa}\cdot\hat{\boldsymbol{n}}=\mathbf{0}$. The normal components of Eq. (2.1) are

$$\begin{cases} i(\hat{\boldsymbol{n}}\times\boldsymbol{\lambda})\cdot\boldsymbol{E}_\parallel=\partial_\tau(\eta_0H_n+\boldsymbol{a}_m*\eta_0\boldsymbol{H}_\parallel+c_m*\eta_0H_n), \\ i(\hat{\boldsymbol{n}}\times\boldsymbol{\lambda})\cdot\eta_0\boldsymbol{H}_\parallel=-\partial_\tau(E_n+\boldsymbol{a}_e*\boldsymbol{E}_\parallel+c_e*E_n). \end{cases}$$

In order to eliminate E_n and H_n, introduce the resolvents L_e and L_m defined by the resolvent equations

$$c_\kappa+L_\kappa+c_\kappa*L_\kappa=0,\quad \kappa=e,m. \tag{3.2}$$

This implies that the normal components of the fields can be expressed in the parallel components of the electric and the magnetic fields.

$$\begin{cases} E_n=-(1+L_e*)[i\partial_\tau^{-1}(\hat{\boldsymbol{n}}\times\boldsymbol{\lambda})\cdot\eta_0\boldsymbol{H}_\parallel+\boldsymbol{a}_e*\boldsymbol{E}_\parallel] \\ \eta_0H_n=(1+L_m*)[i\partial_\tau^{-1}(\hat{\boldsymbol{n}}\times\boldsymbol{\lambda})\cdot\boldsymbol{E}_\parallel-\boldsymbol{a}_m*\eta_0\boldsymbol{H}_\parallel] \end{cases}$$

where the anti-derivative is $\partial_\tau^{-1}f(\tau)=\int_{-\infty}^{\tau}f(\tau')d\tau'$. Insert this equation into the parallel components of Eq. (2.1) given above. The result is an equation in only the parallel components of the electric and the magnetic fields.

$$\partial_n\begin{pmatrix}\boldsymbol{E}_\parallel\\ \hat{\boldsymbol{n}}\times\eta_0\boldsymbol{H}_\parallel\end{pmatrix}=\left[\begin{pmatrix}\mathbf{0}&\boldsymbol{\Gamma}_1\\ \boldsymbol{\Gamma}_2&\mathbf{0}\end{pmatrix}+\begin{pmatrix}\mathbf{D}_{ee}&\mathbf{D}_{em}\\ \mathbf{D}_{me}&\mathbf{D}_{mm}\end{pmatrix}*\partial_\tau\right]\begin{pmatrix}\boldsymbol{E}_\parallel\\ \hat{\boldsymbol{n}}\times\eta_0\boldsymbol{H}_\parallel\end{pmatrix} \tag{3.3}$$

Here two new dyadics are defined

$$\boldsymbol{\Gamma}_1=\mathbf{I}_\parallel\partial_\tau+\boldsymbol{\lambda}\boldsymbol{\lambda}\partial_\tau^{-1},\qquad \boldsymbol{\Gamma}_2=\mathbf{I}_\parallel\partial_\tau+(\hat{\boldsymbol{n}}\times\boldsymbol{\lambda})(\hat{\boldsymbol{n}}\times\boldsymbol{\lambda})\partial_\tau^{-1},$$

and $\mathbf{D}_{\kappa\lambda}$ are the two-dimensional dyadics

$$\begin{cases} \mathbf{D}_{ee} = i[(1 + L_e*)\boldsymbol{\lambda}\boldsymbol{a}_e + (1 + L_m*)(\hat{\boldsymbol{n}} \times \boldsymbol{b}_m)(\hat{\boldsymbol{n}} \times \boldsymbol{\lambda})]\partial_\tau^{-1}, \\ \mathbf{D}_{me} = [\boldsymbol{\chi}_{\parallel,e} - \boldsymbol{b}_e * (1 + L_e*)\boldsymbol{a}_e] + L_m(\hat{\boldsymbol{n}} \times \boldsymbol{\lambda})(\hat{\boldsymbol{n}} \times \boldsymbol{\lambda})\partial_\tau^{-2}, \\ \mathbf{D}_{em} = -[\hat{\boldsymbol{n}} \times \boldsymbol{\chi}_{\parallel,m} \times \hat{\boldsymbol{n}} + (\hat{\boldsymbol{n}} \times \boldsymbol{b}_m) * (1 + L_m*)(\hat{\boldsymbol{n}} \times \boldsymbol{a}_m)] + L_e\boldsymbol{\lambda}\boldsymbol{\lambda}\partial_\tau^{-2}, \\ \mathbf{D}_{mm} = i[(1 + L_m*)(\hat{\boldsymbol{n}} \times \boldsymbol{\lambda})(\hat{\boldsymbol{n}} \times \boldsymbol{a}_m) + (1 + L_e*)\boldsymbol{b}_e\boldsymbol{\lambda}]\partial_\tau^{-1}. \end{cases} \tag{3.4}$$

Notice that in the following all vectors and dyadics are two-dimensional and normal to $\hat{\boldsymbol{n}}$.

4 Wave splitting

The wave splitting transformation is a change of the dependent variables $\boldsymbol{E}_\parallel$ and $\boldsymbol{H}_\parallel$ to a new pair of fields $\boldsymbol{F}^\pm$. Physically, these new fields can be interpreted as a decomposition of the the original fields with respect to the location of their sources. Specifically, the wave splitting diagonalizes Eq. (3.3) in vacuum.

The appropriate splitting, used in this paper, is determined by the principal part of Eq. (3.3). Introduce the Neumann to Dirichlet operator $\mathcal{K}$, cf. [47, 51], that maps Neumann data on a plane $n = n_0$ to Dirichlet data on this plane, and its inverse $\mathcal{K}^{-1}$. These operators satisfy the relations

$$\begin{cases} \mathcal{K}^{-1} = [\partial_\tau^2 + \lambda^2]\mathcal{K}, \\ (\boldsymbol{\Gamma}_2\mathcal{K})(\mathcal{K}\boldsymbol{\Gamma}_1) = \mathbf{I}_\parallel, \\ \boldsymbol{\Gamma}_1 = -\hat{\boldsymbol{n}} \times \boldsymbol{\Gamma}_2 \times \hat{\boldsymbol{n}}, \\ \mathcal{K}\boldsymbol{\Gamma}_i = \boldsymbol{\Gamma}_i\mathcal{K} \qquad i = 1, 2. \end{cases} \tag{4.1}$$

Note that

$$\boldsymbol{\Gamma}_1 \cdot \boldsymbol{\Gamma}_2 = \boldsymbol{\Gamma}_2 \cdot \boldsymbol{\Gamma}_1 = \mathbf{I}_\parallel[\partial_\tau^2 + \lambda^2].$$

Explicit integral representations of the operators $\mathcal{K}$, $\mathcal{K}^2$ and $\mathcal{K}^{-1}$ are derived in Ref. 47 in $((\boldsymbol{r}, t))$ space, and in Ref. 20 in $(\boldsymbol{\lambda}, n, \tau)$ space. The integral representations are

$$\begin{cases} \mathcal{K}\boldsymbol{F} = K * \boldsymbol{F}, \\ \mathcal{K}^{-1}\boldsymbol{F} = (\partial_\tau + L*)\boldsymbol{F}, \\ \mathcal{K}^2\boldsymbol{F} = M * \boldsymbol{F}, \end{cases} \tag{4.2}$$

Throughout this paper operators are typed in Calligraphic font and the corresponding integral kernels are typed in Italic font. The integral kernels K, L and M are obtained using either a Laplace transform technique, see Ref. 20, or applying the two-dimensional Fourier transform to the results in Ref. 47, see Appendix A. The results are

$$\begin{cases} K(\lambda, \tau) = H(\tau)J_0(\lambda\tau), \\ L(\lambda, \tau) = H(\tau)\lambda\dfrac{J_1(\lambda\tau)}{\tau}, \\ M(\lambda, \tau) = H(\tau)\dfrac{\sin(\lambda\tau)}{\lambda}, \end{cases} \tag{4.3}$$

where $H(\tau)$ denotes the Heaviside step function. The integral representation of the combined operators $\mathcal{K}\boldsymbol{\Gamma}_1$ and $\boldsymbol{\Gamma}_2\mathcal{K}$ are obtained from the rule

$$\partial_\tau \mathcal{K} = K(0^+) + K_\tau * , \tag{4.4}$$

where K_τ denotes partial differentiation of the kernel K with respect to τ. All operators act successively from the right to the left, i.e.,

$$\partial_\tau \mathcal{K}\boldsymbol{F} = \partial_\tau(\mathcal{K}\boldsymbol{F}).$$

In vacuum, the parallel field components satisfy the Klein-Gordon equations

$$\left(\partial_n^2 - \partial_\tau^2 - \lambda^2\right)\boldsymbol{E}_\parallel = \left(\partial_n^2 - \partial_\tau^2 - \lambda^2\right)(\hat{\boldsymbol{n}} \times \eta_0 \boldsymbol{H}_\parallel) = \boldsymbol{0}.$$

Consider the canonical half space problem in vacuum with sources to the left (right) of n_0. In the region $n > n_0$ ($n < n_0$) the parallel field components satisfy the Klein-Gordon equation, and at the boundary $n = n_0$ the fields satisfy the up-going (down-going) boundary condition

$$\boldsymbol{E}_\parallel \pm \mathcal{K}\boldsymbol{\Gamma}_1 \hat{\boldsymbol{n}} \times \eta_0 \boldsymbol{H}_\parallel = \boldsymbol{0}.$$

These up-going and down-going conditions are derived in Refs 47,51. Note also that the relation $\partial_n \boldsymbol{E}_\parallel = \boldsymbol{\Gamma}_1 \cdot (\hat{\boldsymbol{n}} \times \eta_0 \boldsymbol{H}_\parallel)$ holds in vacuum. The up-going and down-going conditions lead to the definition of the wave splitting transformation

$$\boldsymbol{F}^\pm = \frac{1}{2}(\boldsymbol{E}_\parallel \mp \mathcal{K}\boldsymbol{\Gamma}_1 \hat{\boldsymbol{n}} \times \eta_0 \boldsymbol{H}_\parallel),$$

with the inverse

$$\begin{pmatrix} \boldsymbol{E}_\parallel \\ \hat{\boldsymbol{n}} \times \eta_0 \boldsymbol{H}_\parallel \end{pmatrix} = \begin{pmatrix} \mathbf{I}_\parallel & \mathbf{I}_\parallel \\ -\boldsymbol{\Gamma}_2\mathcal{K} & \boldsymbol{\Gamma}_2\mathcal{K} \end{pmatrix} \begin{pmatrix} \boldsymbol{F}^+ \\ \boldsymbol{F}^- \end{pmatrix}. \tag{4.5}$$

Note that $\boldsymbol{F}^+ + \boldsymbol{F}^- = \boldsymbol{E}_\parallel$. It is easy to verify that the split fields $\boldsymbol{F}^\pm$ satisfy the PDE

$$\begin{pmatrix} (\partial_n + \mathcal{K}^{-1})\boldsymbol{F}^+ \\ (\partial_n - \mathcal{K}^{-1})\boldsymbol{F}^- \end{pmatrix} = \begin{pmatrix} \boldsymbol{\Delta}_{11} & \boldsymbol{\Delta}_{12} \\ \boldsymbol{\Delta}_{21} & \boldsymbol{\Delta}_{22} \end{pmatrix} * \partial_\tau \begin{pmatrix} \boldsymbol{F}^+ \\ \boldsymbol{F}^- \end{pmatrix}. \tag{4.6}$$

and the coefficients are given by

$$\begin{pmatrix} \boldsymbol{\Delta}_{11} \\ -\boldsymbol{\Delta}_{12} \\ \boldsymbol{\Delta}_{21} \\ \boldsymbol{\Delta}_{22} \end{pmatrix} = \mathcal{U} \begin{pmatrix} (\mathcal{K}\boldsymbol{\Gamma}_1)\mathbf{D}_{me} \\ \mathbf{D}_{ee} \\ (\mathcal{K}\boldsymbol{\Gamma}_1)\mathbf{D}_{mm}(\boldsymbol{\Gamma}_2\mathcal{K}) \\ -\mathbf{D}_{em}(\boldsymbol{\Gamma}_2\mathcal{K}) \end{pmatrix} \tag{4.7}$$

where

$$\mathcal{U} = \mathcal{U}^{-1} = \frac{1}{2}\begin{pmatrix} -1 & 1 & 1 & 1 \\ 1 & -1 & 1 & 1 \\ 1 & 1 & -1 & 1 \\ 1 & 1 & 1 & -1 \end{pmatrix}. \tag{4.8}$$

Due to Eq. (4.8) and the relations satisfied by $\mathcal{K}$, $\mathcal{K}^{-1}$, $\boldsymbol{\Gamma}_1$ and $\boldsymbol{\Gamma}_2$, there is a 1–1 correspondence between the coefficients $\boldsymbol{\Delta}_{kl}$ of Eq. (4.6) and $\mathbf{D}_{\kappa\lambda}$ of Eq. (3.3).

5 Energy flow

In the previous section, the wave splitting transformation was introduced. This transformation partitions the electromagnetic field with respect to the location of its sources. For plane waves obliquely impinging on the slab, the split fields correspond to electromagnetic fields propagating in the $\pm\hat{\boldsymbol{n}}$ directions, respectively. In this paper, however, the sources are general, and this simple picture breaks down. To see the effects of the splitting in this case, examine the total electromagnetic energy flow through the plane $n = n_0$ up to a given time τ.

Calculate the total energy flow $W(n_0, \tau)$ through the surface $n = n_0$

$$\begin{aligned} W(n_0,\tau) &= \iint_{\mathbb{R}^2} \int_{-\infty}^{\tau} \hat{\boldsymbol{n}} \cdot [\boldsymbol{E} \times \boldsymbol{H}](\boldsymbol{\rho}, n_0, \tau') d\tau' d\boldsymbol{\rho} \\ &= \frac{1}{4\pi^2\eta_0} \iint_{\mathbb{R}^2} \int_{-\infty}^{\tau} (\boldsymbol{F}^+ + \boldsymbol{F}^-)(\boldsymbol{\lambda}, n_0, \tau') \cdot (\boldsymbol{\Gamma}_2 \mathcal{K})(\overline{\boldsymbol{F}}^+ - \overline{\boldsymbol{F}}^-)(\boldsymbol{\lambda}, n_0, \tau') d\boldsymbol{\lambda} d\tau'. \end{aligned}$$

Here, the bar denotes complex conjugate. Introduce the dyadic-valued kernel $\mathbf{G}$

$$\mathbf{G}(\boldsymbol{\lambda}, \tau) = \delta(\tau)\mathbf{I}_\parallel + \frac{1}{2} f(\lambda, |\tau|)\mathbf{I}_\parallel + \frac{1}{2} g(\lambda, |\tau|)(\hat{\boldsymbol{n}} \times \boldsymbol{\lambda})(\hat{\boldsymbol{n}} \times \boldsymbol{\lambda}),$$

where (cf. Eqs (4.4) and (4.3))

$$\begin{cases} f(\lambda,\tau) = H(\tau)\partial_\tau J_0(\lambda\tau) = -H(\tau)\lambda J_1(\lambda\tau), \\ g(\lambda,\tau) = H(\tau) \displaystyle\int_0^\tau J_0(\lambda\tau')\, d\tau', \end{cases}$$

Note that $\mathbf{G}$ is a real and symmetric dyadic, and, furthermore, by construction it is an even distribution in time. Define the energy flow density w

$$W(n_0,\tau) = \frac{1}{4\pi^2\eta_0} \iint_{\mathbb{R}^2} w(\boldsymbol{\lambda}, n_0, \tau) d\boldsymbol{\lambda}.$$

This energy flow density w is given in terms of the dyadic-valued kernel $\mathbf{G}$ as

$$\begin{aligned} w(\boldsymbol{\lambda}, n_0, \tau) = &\int_{-\infty}^{\tau} \int_{-\infty}^{\tau} \boldsymbol{F}^+(\boldsymbol{\lambda}, n_0, \tau') \cdot \mathbf{G}(\boldsymbol{\lambda}, \tau' - \tau'') \cdot \overline{\boldsymbol{F}}^+(\boldsymbol{\lambda}, n_0, \tau'') d\tau' d\tau'' \\ &- \int_{-\infty}^{\tau} \int_{-\infty}^{\tau} \boldsymbol{F}^-(\boldsymbol{\lambda}, n_0, \tau') \cdot \mathbf{G}(\boldsymbol{\lambda}, \tau' - \tau'') \cdot \overline{\boldsymbol{F}}^-(\boldsymbol{\lambda}, n_0, \tau'') d\tau' d\tau'' \\ &+ w_{\text{mixed}}(\boldsymbol{\lambda}, n_0, \tau). \end{aligned}$$

The contribution to $W(n_0, \tau)$ due to w_{mixed} is zero. To see this, apply the inverse splitting, (4.5), and the inverse Fourier transform back to the electromagnetic fields

$\boldsymbol{E}_\parallel((\boldsymbol{r},t))$ and $\boldsymbol{H}_\parallel((\boldsymbol{r},t))$. In $(\boldsymbol{\lambda},n,\tau)$ space, this leads to the constraint

$$\iint\limits_{\mathbb{R}^2}\int\limits_{-\infty}^{\tau}\int\limits_{-\infty}^{\tau'}\boldsymbol{F}^-(\boldsymbol{\lambda},n_0,\tau')\cdot\mathbf{G}(\boldsymbol{\lambda},\tau'-\tau'')\cdot\overline{\boldsymbol{F}}^+(\boldsymbol{\lambda},n_0,\tau'')d\tau'd\tau''d\boldsymbol{\lambda}$$
$$=\iint\limits_{\mathbb{R}^2}\int\limits_{-\infty}^{\tau}\int\limits_{-\infty}^{\tau'}\boldsymbol{F}^+(\boldsymbol{\lambda},n_0,\tau')\cdot\mathbf{G}(\boldsymbol{\lambda},\tau'-\tau'')\cdot\overline{\boldsymbol{F}}^-(\boldsymbol{\lambda},n_0,\tau'')d\tau'd\tau''d\boldsymbol{\lambda}$$

in the split fields $\boldsymbol{F}^\pm(\boldsymbol{\lambda},n_0,\tau)$. Note, however, that $w_{\text{mixed}}(\boldsymbol{\lambda},n_0,\tau)$ is not zero in general.

To see the effect of the non-vanishing terms study the sign of the integral

$$\int\limits_{-\infty}^{\tau}\int\limits_{-\infty}^{\tau}\boldsymbol{F}(\tau')\cdot\mathbf{G}(\boldsymbol{\lambda},\tau'-\tau'')\cdot\overline{\boldsymbol{F}}(\tau'')d\tau'd\tau''$$

Consider the eigenvalues of $\mathbf{G}$

$$g_1(\lambda,\tau)=\delta(\tau)+\frac{1}{2}f(\lambda,|\tau|),$$
$$g_2(\lambda,\tau)=\delta(\tau)+\frac{1}{2}f(\lambda,|\tau|)+\frac{\lambda^2}{2}g(\lambda,|\tau|),$$

with eigenvectors $\boldsymbol{\lambda}$ and $\hat{\boldsymbol{n}}\times\boldsymbol{\lambda}$, respectively. The eigenvalues are even distributions in τ. The cosine transforms are

$$\int\limits_0^\infty\cos(\xi\tau)g_1(\lambda,\tau)d\tau=H(|\xi|-\lambda)\frac{|\xi|}{2\sqrt{\xi^2-\lambda^2}},$$
$$\int\limits_0^\infty\cos(\xi\tau)g_2(\lambda,\tau)d\tau=H(|\xi|-\lambda)\frac{\sqrt{\xi^2-\lambda^2}}{2|\xi|}+\frac{\pi\lambda}{2}\delta(\xi),$$

which are even, positive distributions of ξ. This implies that $\mathbf{G}$ is a dyadic of positive type (slightly generalized Bochner-Schwartz' theorem, cf. Ref. 43) and therefore

$$\int\limits_{-\infty}^{\tau}\int\limits_{-\infty}^{\tau}\boldsymbol{F}(\tau')\cdot\mathbf{G}(\tau'-\tau'')\cdot\overline{\boldsymbol{F}}(\tau'')d\tau'd\tau''\geq 0.$$

Hence, positive or negative contributions to $w(\boldsymbol{\lambda},n_0,\tau)$ and $W(n_0,\tau)$ arise from $\boldsymbol{F}^+$ or $\boldsymbol{F}^-$, respectively, irrespective of the excitation of the slab and the time τ.

6 Wave propagators

Both the direct and the inverse problem are solved using scattering operators [13, 15]. These operators map the incident field to the scattered transmitted and reflected

field, respectively. One important property of these operators is that they depend only on the material of the slab and not on the incident field. In previous work [16, 35, 37], the scattering operators are calculated using Green functions or the imbedding method. In the imbedding method the basic tool is the scattering operators for a sub-slab. A variation of one of the edges of the sub-slab leads to the imbedding equations for the scattering operators. Both the Green functions approach and the imbedding method are connected to each other via Volterra equations of the second kind [16, 37]. This suggests a unified approach and the corresponding scattering operators are called wave propagators [25, 27].

Consider the case when the sources of the field is in the region $n < 0$. Let $n \in [n_1, n_2] \subseteq [0, d]$ and define for the field $\boldsymbol{F}^+(n_1, \tau)$ the propagators $\mathcal{P}^{++}$ and $\mathcal{P}^{-+}$

$$\begin{cases} \boldsymbol{F}^+(n_2, \tau + (n_2 - n_1)) = \mathcal{P}^{++}(n_2, n_1)\boldsymbol{F}^+(n_1, \tau), \\ \boldsymbol{F}^-(n_2, \tau + (n_2 - n_1)) = \mathcal{P}^{-+}(n_2, n_1)\boldsymbol{F}^+(n_1, \tau). \end{cases} \tag{6.1}$$

If the sources are located in the region $n > d$ propagators for $\boldsymbol{F}^-(n_2, \tau)$ are defined analogously. Note that for $n_1 > n_2$ the field is propagated backwards in time. In this case the wave propagators are analogous to the Green functions used in Ref. 18.

The propagators satisfy the composition rules (+-case)

$$\begin{cases} \mathcal{P}^{++}(n_2, n_1) = \mathcal{P}^{++}(n_2, n)\mathcal{P}^{++}(n, n_1) \\ \mathcal{P}^{-+}(n_2, n_1) = \mathcal{P}^{-+}(n_2, n_2)\mathcal{P}^{++}(n_2, n_1) \\ \mathcal{P}^{++}(n_1, n_1) = \mathcal{I} \end{cases} \tag{6.2}$$

for all n, and where $\mathcal{I}$ is the identity operator. The middle rule motivates the introduction of a reflection operator

$$\mathcal{R}^+(n) = \mathcal{P}^{-+}(n, n).$$

Note that the sub-slab $[n_1, n_2]$ is imbedded in the physical slab, i.e., the sub-slab $[n_1, n_2]$ is sandwiched between $[0, \min_i n_i]$ and $[\max_i n_i, d]$. This assumption is crucial for the simplicity of the composition rules, (6.2), cf. the Redheffer star product technique wherein the scattering operators are defined for a sub-slab imbedded in vacuum [42]. The composition rules (6.2) are generalizations of the previously obtained relations between the imbedding and Green functions methods, see Ref. 16 and Appendix B.

6.1 Alternative dynamics

Introduce $\boldsymbol{F}^- = \mathcal{R}^+\boldsymbol{F}^+$ on the right hand side in Eq. (4.6). Formally, the result is

$$(\partial_n \pm \partial_\tau)\boldsymbol{F}^\pm = \mathcal{A}^{\pm+}\boldsymbol{F}^+, \tag{6.3}$$

where $\mathcal{A}^{\pm+} = \partial_\tau \mathbf{A}^{\pm+}*$, cf. (4.4), and

$$\begin{aligned} \mathbf{A}^{++} &= -\partial_\tau^{-1}\mathbf{L} + \boldsymbol{\Delta}_{11} + \boldsymbol{\Delta}_{12} * \mathbf{R}^+, \\ \mathbf{A}^{-+} &= \partial_\tau^{-1}\mathbf{L} + \boldsymbol{\Delta}_{21} + \boldsymbol{\Delta}_{22} * \mathbf{R}^+. \end{aligned}$$

Here the representation[1] $\mathcal{R}^+ = \mathbf{R}^+*$ is used and $\mathbf{L} = L\mathbf{I}_\parallel$, see Eqs. (4.2) and (4.3).

6.2 Reflection operator

If $n_1 = n_2 = n$ in the second equation of (6.1), the following PDE for the reflection operator $\mathcal{R}^+$ is obtained by differentiating wrt n and repeated use of (6.3):

$$\mathcal{R}^+_n - 2\partial_\tau \mathcal{R}^+ = \mathcal{A}^{-+} - \mathcal{R}^+ \mathcal{A}^{++}.$$

Balancing multiplicative and convolution parts in this equation, cf. Eq (4.4), yields

$$\mathbf{R}^+(n, 0^+) = -\frac{1}{2}\mathbf{\Delta}_{21}(n, 0^+), \tag{6.4}$$

$$(\partial_n - 2\mathcal{K}^{-1})\mathbf{R}^+ = \partial_\tau(\mathbf{\Delta}_{21} + \mathbf{\Delta}_{22} * \mathbf{R}^+ - \mathbf{R}^+ * \mathbf{\Delta}_{11} - \mathbf{R}^+ * \mathbf{\Delta}_{12} * \mathbf{R}^+). \tag{6.5}$$

For a finite slab the reflection kernel vanishes on the rear side, i.e.,

$$\mathbf{R}^+(d, \tau) \equiv \mathbf{0}. \tag{6.6}$$

Therefore a finite jump-discontinuity propagates along the characteristic of the PDE in (6.5). The exact form is derived in Ref. 16

$$[\mathbf{R}^+(n, 2(d-n))]^+_- = \frac{1}{2}\mathbf{Q}^-(d, n)\mathbf{\Delta}_{21}(d, 0^+)\mathbf{Q}^+(n, d). \tag{6.7}$$

Here, the dyadics $\mathbf{Q}^\pm$ are the wave front propagators, see Appendix B or Ref. 16.

6.3 Transmission operator

The following PDEs are obtained from Eqs (6.1) and (6.3)[2]:

$$\begin{cases} \mathcal{P}^{++}_{n_2}(n_2, n_1) = \mathcal{A}^{++}(n_2)\mathcal{P}^{++}(n_2, n_1), \\ \mathcal{P}^{++}_{n_1}(n_2, n_1) = -\mathcal{P}^{++}(n_2, n_1)\mathcal{A}^{++}(n_1). \end{cases} \tag{6.8}$$

Integration of these equations gives integral equations of the following kind:

$$\mathcal{P}^{++}(n_2, n_1) = \mathcal{I} + \int_{n_1}^{n_2} \mathcal{A}^{++}(n)\mathcal{P}^{++}(n, n_1)dn = \mathcal{I} + \int_{n_1}^{n_2} \mathcal{P}^{++}(n_2, n)\mathcal{A}^{++}(n)dn.$$

The unique solution to these integral equations is [5, p. 177-178]

$$\mathcal{P}^{++}(n_2, n_1) = \mathcal{S} \exp\left(\int_{n_1}^{n_2} \mathcal{A}^{++}(n)dn\right), \tag{6.9}$$

Here a spatial ordering operator $\mathcal{S}$ is used. By definition

$$\mathcal{S}[\mathcal{A}(n_1)\mathcal{A}(n_2)\dots\mathcal{A}(n_k)] = \mathcal{A}(\max_i n_i)\dots\mathcal{A}(\min_i n_i),$$

[1] This representation is justified from the absence of jump-discontinuities in $\boldsymbol{F}^-$ along the characteristic of $\boldsymbol{F}^+$.

[2] Note that ∂_τ commutes with $\partial_\tau \mathbf{A}^{++}*$.

where the operators on the right hand side have been arranged in order of decreasing arguments n_i. Note that the operator $\mathcal{A}^{++}$ is the generator of a semi-group.

The solution (6.9) comprises the wave front propagator and the transmission kernel or the Green function used in Refs 15, 16. For the connection to these techniques, see Appendix B. An analogous result using fixed frequency methods is found in Ref. 3.

To further analyze the properties of the solution (6.9) define the generator $\mathcal{A}$ and the corresponding propagator $\mathcal{P}$, i.e.,

$$\mathcal{P}(n_2, n_1) = \mathcal{S} \exp\left(\int_{n_1}^{n_2} \mathcal{A}(n, \tau) dn \right).$$

It is useful to decompose the generator as $\mathcal{A}(n) = \mathcal{B}(n) + \mathcal{C}(n)$ and define

$$\mathcal{P}_B(n_2, n_1) = \mathcal{S} \exp\left(\int_{n_1}^{n_2} \mathcal{B}(n, \tau) dn \right).$$

The propagator $\mathcal{P}(n_2, n_1)$ can be factored in two ways

$$\mathcal{P}(n_2, n_1) = \mathcal{P}_B(n_2, n_1)\mathcal{P}_{\mathrm{R}}(n_2, n_1) = \mathcal{P}_{\mathrm{L}}(n_2, n_1)\mathcal{P}_B(n_2, n_1).$$

The operators $\mathcal{P}_{\mathrm{R,L}}$ are obtained by using Equations (6.8) and (6.2). The solutions are

$$\begin{cases} \mathcal{P}_{\mathrm{R}}(n_2, n_1) = \mathcal{S} \exp\left(\int_{n_1}^{n_2} \mathcal{P}_B(n_1, n)\mathcal{C}(n)\mathcal{P}_B(n, n_1) dn \right), \\ \mathcal{P}_{\mathrm{L}}(n_2, n_1) = \mathcal{S} \exp\left(\int_{n_1}^{n_2} \mathcal{P}_B(n_2, n)\mathcal{C}(n)\mathcal{P}_B(n, n_2) dn \right). \end{cases} \tag{6.10}$$

6.4 The Sommerfeld forerunner

On a small enough time scale after the arrival of the wave front, it is possible to approximate the response of the medium, and to derive an explicit expression of the transmission operator. The associated propagator is, by definition, the Sommerfeld propagator and the related field is the Sommerfeld precursor or forerunner [7].

The early time behavior of the field is approximated by evaluating the generator at $\tau = 0^+$. This defines the generator $\mathcal{A}^{++}$

$$\mathcal{A}_{\mathrm{S}}^{++}(n) = \mathbf{A}^{++}(n, 0^+) + \mathbf{A}_{\tau}^{++}(n, 0^+) * ,$$

which, by definition, is the generator of the Sommerfeld propagator, i.e.,

$$\mathcal{P}_{\mathrm{S}}^{++}(n_2, n_1) = \mathcal{S} \exp\left(\int_{n_1}^{n_2} \mathcal{A}_{\mathrm{S}}^{++}(n) dn \right).$$

This expression can be rewritten using Eq. (6.10). The result is

$$\mathcal{P}_{\mathrm{S}}^{++}(n_2, n_1) = \mathbf{Q}^{+}(n_1, n_2)\mathcal{S} \exp\left(-\mathbf{B}(n_2, n_1) * \right),$$

where

$$\mathbf{B}(n_2, n_1) = -\int_{n_1}^{n_2} \mathbf{Q}^+(n_1, n)\mathbf{A}_\tau^{++}(n, 0^+)\mathbf{Q}^+(n, n_1)dn \tag{6.11}$$

and $\mathbf{Q}^+$ is the wave front propagator, cf. Appendix B. The convolution part of the Sommerfeld propagator simplifies according to the formal rule

$$(1*)^k = \frac{\tau^{k-1}}{(k-1)!} * .$$

This implies then

$$\mathcal{P}_{\mathrm{S}}^{++}(n_2, n_1) = \mathbf{Q}^+(n_2, n_1)\left[\mathbf{I}_\parallel - \mathcal{S}\sqrt{\frac{\mathbf{B}(n_2, n_1)}{\tau}}J_1\left(2\sqrt{\tau\mathbf{B}(n_2, n_1)}\right)*\right],$$

where the power series expansion of the Bessel function of first order J_1 has been employed. Clearly this result is a generalization of previously obtained results for isotropic and bi-isotropic media [45]. Note that the above result holds for any medium where the combined Maxwell equations and constitutive relations can be cast in the form of Eq. (4.6). Therefore, it is a straightforward procedure to calculate the forerunner in the plane wave case [15] or for a bi-anisotropic dispersive medium [14]. In Appendix C, the Sommerfeld forerunner is further investigated and the exact conditions, under which the forerunner is the dominant contribution to the electromagnetic field, are given.

7 The inverse problem for homogeneous media

The inverse scattering problem for homogeneous anisotropic media can be solved using plane waves [15]. The inversion algorithm is based upon a technique similar to solving a Volterra integral equation of the second kind. This method uses the Green functions evaluated at all points $n \in [0, d]$. However, by employing the exact solution, (6.9), the use of Green functions becomes obsolete and the inversion algorithm only requires reflection data $\mathbf{R}^+(n, \tau)$ at $n \in [0, d]$. An even simpler algorithm is obtained for susceptibility dyadics with homogeneous initial values, i.e., $\boldsymbol{\chi}_e(0^+) = \boldsymbol{\chi}_m(0^+) = \mathbf{0}$. This implies that $\boldsymbol{\Delta}_{kl}(0^+) = \mathbf{0}$. This is a relevant and physical assumption, cf. Ref. 23, and an example of such a medium is the Lorentz medium, see Ref. 6, where each component of the susceptibility dyadics $\boldsymbol{\chi}_e$ and $\boldsymbol{\chi}_m$ is a sum of exponentially attenuated sinusoidal functions of time. In the subsections 7.1 and 7.2 it is assumed that the susceptibility dyadics have homogeneous initial values, i.e., $\boldsymbol{\chi}_e(0^+) = \boldsymbol{\chi}_m(0^+) = \mathbf{0}$, or $\boldsymbol{\Delta}_{kl}(0^+) = \mathbf{0}$.

7.1 Reflection data inversion

Consider the triangular region in space-time, n-τ, bounded by the lines $\tau = 0$, $n = 0$ and $\tau = 2(d - n)$. In this region the reflection kernel $\mathbf{R}^+$ is independent of n, since, due to causality, the medium is effectively semi-infinite, and the effects of the back

wall have not arrived yet. Therefore, in this region the reflection kernel $\mathbf{R}^+(n,\tau)$ is identical to the reflection kernel $\mathbf{R}_\infty(\tau)$ of the semi-infinite slab ($d \to \infty$). To make use of this property of the reflection kernel $\mathbf{R}^+$, the time delay operator is used. Explicitly

$$\delta_a \mathbf{A}(\tau) = \delta(\tau - a) * \mathbf{A}(\tau) = \mathbf{A}(\tau - a).$$

Here, δ_a denotes the time delay operator with delay a and the delta function $\delta(\tau - a)$ is the kernel in the integral representation. Now decompose the reflection kernel as

$$\mathbf{R}^+(n,\tau) = \mathbf{R}_\infty(\tau) - \delta_{2(d-n)}\mathbf{R}_\infty(\tau) + \mathbf{R}_0(n,\tau).$$

The first kernel $\mathbf{R}_\infty(\tau)$ comprises only pure medium response, i.e., no scattering effects from the back wall which are contained in the second and third kernels in this decomposition. Due to causality

$$\begin{cases} \mathbf{R}_\infty(\tau) = \mathbf{0} \text{ for } \tau < 0, \\ \mathbf{R}_0(n,\tau) = \mathbf{0} \text{ for } \tau < 2(d-n). \end{cases}$$

By definition the kernel $\mathbf{R}_\infty$ satisfies

$$2\mathbf{R}_\infty + \mathbf{\Delta}_{21} = -\partial_\tau^{-1} 2\mathbf{L} * \mathbf{R}_\infty - \mathbf{\Delta}_{22} * \mathbf{R}_\infty + \mathbf{R}_\infty * \mathbf{\Delta}_{11} + \mathbf{R}_\infty * \mathbf{\Delta}_{12} * \mathbf{R}_\infty, \tag{7.1}$$

which implies that the kernel $\mathbf{R}_0$ satisfies

$$(\partial_n - 2\partial_\tau)\mathbf{R}_0 = \mathbf{\Sigma}_{21} + \mathbf{\Sigma}_{22} * \mathbf{R}_0 - \mathbf{R}_0 * \mathbf{\Sigma}_{11} - \mathbf{R}_0 * \mathbf{\Sigma}_{12} * \mathbf{R}_0, \tag{7.2}$$

cf. Eq. (6.5). The explicit forms of the kernels $\mathbf{\Sigma}_{kl}$ are

$$\begin{cases} \mathbf{\Sigma}_{21} = -\delta_{2(d-n)}\big[(\mathbf{\Delta}'_{22} + 2\mathbf{L}) * \mathbf{R}_\infty - \mathbf{R}_\infty * \mathbf{\Delta}'_{11} \\ \qquad\qquad - (2 - \delta_{2(d-n)})\mathbf{R}_\infty * \mathbf{\Delta}'_{12} * \mathbf{R}_\infty\big], \\ \mathbf{\Sigma}_{22} = \mathbf{\Delta}'_{22} + 2\mathbf{L} - (1 - \delta_{2(d-n)})\mathbf{R}_\infty * \mathbf{\Delta}'_{12}, \\ \mathbf{\Sigma}_{11} = \mathbf{\Delta}'_{11} + (1 - \delta_{2(d-n)})\mathbf{\Delta}'_{12} * \mathbf{R}_\infty, \\ \mathbf{\Sigma}_{12} = \mathbf{\Delta}'_{12}. \end{cases}$$

The initial and boundary values are

$$\mathbf{R}_\infty(0^+) = \mathbf{0}, \tag{7.3}$$

$$\mathbf{R}_0(d,\tau) = \mathbf{0}, \tag{7.4}$$

$$\mathbf{R}_0(n, 2(d-n)^+) = \mathbf{0}. \tag{7.5}$$

Here Eqs (7.3) and (7.4) follow from Eqs (6.4) and (6.6), respectively, and Eq. (6.7) implies Eq. (7.5).

Evidently, the PDE for $\mathbf{R}_0$ is coupled to the PDE for $\mathbf{R}_\infty$. To decouple them, numerically and time step by time step, use an equidistant time discretization and an integration quadrature that includes the end points of the time interval. Consider the inverse problem and the reconstruction of $\mathbf{\Delta}_{21}(\tau_0)$ using $\mathbf{R}^+(0,\tau_0)$. Due to the initial values $\mathbf{\Delta}_{kl}(0^+) = \mathbf{0}$, only the left hand side members of Eqs (7.1) and (7.2)

depend on τ_0, and the right hand side members are known. Here, it is assumed that the medium parameters are recovered for all earlier times, i.e., $\tau < \tau_0$. This implies that $\mathbf{R}_0(0,\tau_0)$ can be recovered and therefore, by using the indata $\mathbf{R}^+(0,\tau_0)$ the kernel $\mathbf{R}_\infty(\tau_0)$ can be recovered. Thence, the kernel $\mathbf{R}_\infty(\tau_0)$ and Eq. (7.1) can be used to recover $\boldsymbol{\Delta}_{21}(\tau_0)$. To proceed to the next time step more indata is needed, see Subsection 7.2, since the kernels $\boldsymbol{\Delta}_{22}(\tau_0)$, $\boldsymbol{\Delta}_{11}(\tau_0)$ and $\boldsymbol{\Delta}_{12}(\tau_0)$ are needed in the next time step. Note that the kernel $\mathbf{R}_\infty$ corresponding to a semi-infinite medium is used to recover $\boldsymbol{\Delta}_{21}$. Physically, the kernels $\delta_{2(d-n)}\mathbf{R}_\infty(\tau)$ and $\mathbf{R}_0(n,\tau)$ comprise the reflections due to the back wall and these effects obscure the response of the medium. By using the above decomposition, it is possible to identify and to eliminate this problem.

Note, in this subsection it is demonstrated that the kernel $\boldsymbol{\Delta}'_{21}$ can be reconstructed time step by time step if the kernels $\boldsymbol{\Delta}'_{11}$, $\boldsymbol{\Delta}'_{12}$ and $\boldsymbol{\Delta}'_{22}$ can be recovered using other equations.

7.2 Transmission data inversion

In any slab with a homogeneous medium, the propagator $\mathcal{P}^{++}(n_2,n_1)$ depends only on the distance of propagation $n_2 - n_1$, and the distance to the back wall $d - n_2$. This is so, since the propagators are independent of the excitation $\boldsymbol{F}^+(n_1,\tau)$, and therefore any change of the medium in the region $n \in [0,n_1]$ does not affect $\mathcal{P}^{++}(n_2,n_1)$. Note that the propagator is invariant under spatial translations if $d = \infty$ and, in that case, $\mathbf{R}^+ = \mathbf{R}_\infty$ which implies that $\mathcal{S} = \mathcal{I}$. However, in a finite slab the spatial ordering operator is not an identity, since $\mathbf{R}^+$ is a dyadic-valued function of n, and therefore

$$\mathcal{A}^{++}(n')\mathcal{A}^{++}(n'') \neq \mathcal{A}^{++}(n'')\mathcal{A}^{++}(n'),$$

in general. In order to use the solution (6.9), extract the commuting part of the generator $\mathcal{A}^{++}(n)$ and factor the propagator using Eq. (6.10). Explicitly,

$$\begin{cases} \mathcal{P}^{++}(n_2,n_1) = \mathcal{P}^{++}_{\mathrm{sd}}(n_2,n_1)\mathcal{P}^{++}_{\mathrm{nr}}(n_2,n_1)\mathcal{P}^{++}_{\mathrm{r}}(n_2,n_1), \\ \mathcal{P}^{++}_{\mathrm{sd}}(n_2,n_1) = \exp\left(-(n_2-n_1)L*\right), \\ \mathcal{P}^{++}_{\mathrm{nr}}(n_2,n_1) = \exp\left((n_2-n_1)\boldsymbol{\Delta}'_{11}*\right), \\ \mathcal{P}^{++}_{\mathrm{r}}(n_2,n_1) = \mathcal{S}\exp\left(\displaystyle\int_{n_1}^{n_2} \mathcal{A}^{++}_{\mathrm{r}}(n_1,n)\,dn\right), \end{cases}$$

where

$$\mathcal{A}^{++}_{\mathrm{r}}(n_1,n) = \exp\left((n_1-n)\boldsymbol{\Delta}'_{11}*\right)\boldsymbol{\Delta}'_{12} * \mathbf{R}^+(n,\cdot) * \exp\left((n-n_1)\boldsymbol{\Delta}'_{11}*\right).$$

Recall the initial values $\boldsymbol{\Delta}_{kl}(0^+) = \mathbf{0}$. This is a decomposition of the propagator $\mathcal{P}^{++}$ in a scalar part due to spatial dispersion (subscript sd), a reflection-independent part (subscript nr), and a third part containing the reflection kernel $\mathbf{R}^+$. To solve this equation for $\boldsymbol{\Delta}'_{11}$, use an equidistant time discretization and an integration quadrature that includes the end points of the time interval. Due to the initial

value of $\mathbf{\Delta}'_{12} * \mathbf{R}^+$, the generator of the propagator $\mathcal{P}_{\rm r}^{++}$ depends only on $\mathbf{\Delta}_{kl}$ at earlier time steps. Hence, at each time step, the generators of $\mathcal{P}_{\rm r}^{++}$ and $\mathcal{P}_{\rm sd}^{++}$ are known. The inverses of $\mathcal{P}_{\rm r}^{++}$ and $\mathcal{P}_{\rm sd}^{++}$ then yield

$$\mathcal{P}_{\rm nr}^{++}(n_2, n_1) = \mathcal{P}_{\rm sd}^{++}(n_1, n_2)\mathcal{P}^{++}(n_2, n_1)\mathcal{P}_{\rm r}^{++}(n_1, n_2).$$

The right hand side terms contain known operators, time step by time step. This result can now be used to recover $\mathbf{\Delta}'_{11}(\tau_0)$. The formal inverse is

$$\mathbf{\Delta}'_{11}* = \frac{1}{n_2 - n_1} \log \mathcal{P}_{\rm nr}^{++}(n_2, n_1).$$

The logarithm on the right hand side is defined via the representation

$$\mathcal{P}_{\rm nr}^{++} = \mathbf{I}_{\|} + \mathbf{P}(\tau)*$$

and the power series expansion of the function $\log(1 + x)$.

Note, in this subsection it is demonstrated that the kernel $\mathbf{\Delta}'_{11}$ can be reconstructed time step by time step if the kernels $\mathbf{\Delta}'_{21}$, $\mathbf{\Delta}'_{12}$ and $\mathbf{\Delta}'_{22}$ can be recovered using other equations.

7.3 Mirror images and the DIP

In the previous sections, the reconstruction of $\mathbf{\Delta}_{21}(\boldsymbol{\lambda}; \tau)$ and $\mathbf{\Delta}_{11}(\boldsymbol{\lambda}; \tau)$ is investigated. The reconstruction is only possible if the kernels $\mathbf{\Delta}_{12}(\boldsymbol{\lambda}; \tau)$ and $\mathbf{\Delta}_{22}(\boldsymbol{\lambda}; \tau)$ can be reconstructed simultaneously. This can be accomplished by the mirror image transformation[3], see Eqs (3.4) and (4.7)

$$\mathbf{\Delta}_{kl}(-\boldsymbol{\lambda}, \tau) = -\mathbf{\Delta}_{\overline{k}\,\overline{l}}(\boldsymbol{\lambda}, \tau). \tag{7.6}$$

Alternatively, use sources in the region $n > d$, and keep the Fourier parameter $\boldsymbol{\lambda}$ the same. However, the mirror image transformation suggested here uses the same sources, and it is therefore more advantageous from an experimental point of view.

Hence, all four kernels $\mathbf{\Delta}_{kl}$ can be reconstructed by using the scattering data

$$\mathcal{R}^+(\pm\boldsymbol{\lambda}; 0), \qquad \mathcal{P}^{++}(\pm\boldsymbol{\lambda}; d, 0).$$

and the algorithm given in Sections (7.1) and (7.2). This is the Dynamics Inverse Problem (DIP) [15].

7.4 RIP

In the RIP (Retrieval of Internal Parameters) the DIP is assumed to be solved for two non-parallel $\boldsymbol{\lambda}$. The output of the DIP are the kernels $\mathbf{\Delta}'_{kl}(\boldsymbol{\lambda}_i, \tau)$ for $i = 1, 2$.

[3]The notation of dual indices, i.e., $\overline{1} = 2$ and $\overline{2} = 1$, is used here.

Using Eqs (4.7), (4.8) and the operator algebra (4.1), $\mathbf{D}'_{\kappa\lambda}(\boldsymbol{\lambda}_i, \tau)$ for $i = 1, 2$, are obtained. The dyadics $\mathbf{D}'_{ee} \times \hat{\boldsymbol{n}}$, $\hat{\boldsymbol{n}} \times \mathbf{D}'_{me} \times \hat{\boldsymbol{n}}$, $\mathbf{D}'_{em}$ and $\hat{\boldsymbol{n}} \times \mathbf{D}'_{mm}$ are on the form

$$\mathbf{D}'(\boldsymbol{\lambda}) = \begin{cases} \boldsymbol{\beta}_L \boldsymbol{\lambda} + \boldsymbol{\lambda} \boldsymbol{\beta}_R \\ \quad \text{or} \\ \boldsymbol{\alpha} + \gamma \boldsymbol{\lambda} \boldsymbol{\lambda}. \end{cases}$$

These dyadic polynomials are uniquely determined, see Ref. 14, by two $\boldsymbol{\lambda}_i$ such that $\boldsymbol{\lambda}_1 \times \boldsymbol{\lambda}_2 \neq \mathbf{0}$. This means that $\mathbf{D}'_{\kappa\lambda}(\boldsymbol{\lambda}_i)$ (κ, $\lambda = e, m$ and $i = 1, 2$) uniquely determine the parameters γ, $\boldsymbol{\beta}_{L/R}$ and $\boldsymbol{\alpha}$. The explicit forms of these parameters are given by Eq. (3.4). Hence, by direct identification, the following quantities are uniquely determined

$$\begin{cases} \partial_\tau^{-1} L_\kappa, \\ (1 + L_\kappa *) \boldsymbol{a}_\kappa, \\ (1 + L_\kappa *) \boldsymbol{b}_\kappa, \\ \partial_\tau \left[\boldsymbol{\chi}_{\parallel,\kappa} - \boldsymbol{b}_\kappa (1 + L_\kappa *) \boldsymbol{a}_\kappa \right], \end{cases} \qquad \kappa = e,\ m. \tag{7.7}$$

To continue, take the time derivative of the top line to recover L_κ and use the resolvent equation (3.2) to recover c_κ. Operate then with $1 + c_\kappa *$ on the middle lines to retrieve the vectors $\boldsymbol{a}_\kappa$ and $\boldsymbol{b}_\kappa$. Finally, the components $\boldsymbol{\chi}_{\parallel,\kappa}$ can be recovered by integrating the bottom line and subtracting the—by now known—contributions from L_κ, $\boldsymbol{a}_\kappa$ and $\boldsymbol{b}_\kappa$. This completes the algorithm.

8 Reciprocal media

A constraint on the scattering data for reciprocal media is derived. Reciprocity implies that $\boldsymbol{\chi}_{\parallel,\kappa}$ are symmetric, which implies $\boldsymbol{a}_\kappa = \boldsymbol{b}_\kappa$. Hence, see (3.4)

$$\begin{aligned} \mathbf{D}^T_{\kappa\kappa} &= \mathbf{D}_{\overline{\kappa}\,\overline{\kappa}}, \\ \mathbf{D}^T_{\kappa\overline{\kappa}} &= \mathbf{D}_{\kappa\overline{\kappa}}. \end{aligned}$$

Here, T denotes the transpose. This implies, see (4.1) and (4.7)

$$\begin{aligned} {}^T &= \boldsymbol{\Delta}_{kk}, \\ [(\boldsymbol{\Gamma}_2 \mathcal{K}) \boldsymbol{\Delta}_{k\overline{k}} (\mathcal{K} \boldsymbol{\Gamma}_1)]^T &= -\boldsymbol{\Delta}_{\overline{k}k}. \end{aligned}$$

Now apply the transformation in the above left hand side to Eq. (6.5). By noting that ∂_n and $\mathcal{K}^{-1}$ commutes with $\boldsymbol{\Gamma}_2 \mathcal{K}$ and $\mathcal{K} \boldsymbol{\Gamma}_1$ it is straightforward to obtain a PDE for the transformed reflection kernel. This PDE is identical to the PDE for the kernel $\mathbf{R}^+(-\boldsymbol{\lambda}; n, \tau)$, see (7.6). Therefore

$$\mathbf{R}^+(-\boldsymbol{\lambda}; n, \tau) = [(\boldsymbol{\Gamma}_2 \mathcal{K}) \mathbf{R}^+ (\mathcal{K} \boldsymbol{\Gamma}_1)]^T (\boldsymbol{\lambda}; n, \tau).$$

9 Conclusions

The inverse problem of reconstructing the material parameters of a homogeneous, dispersive and anisotropic slab is investigated. This can be done using several plane waves, see Ref. 15. However, in the technique developed here, the inverse problem can be solved by using only one single excitation of the slab, and scattering data corresponding to a finite number of Fourier parameters $\boldsymbol{\lambda}$. The prize paid for this is the need for time differentiation of reconstructed data in order to obtain the susceptibility kernels, see (7.7). Note, however, that the reconstruction does not need the inverse Fourier transformation.

The use of wave propagators provides an exact solution for the transmission operator. Hence, the reconstruction of internal transmission data is obsolete, and the Karlsson method used in Ref. 15 can be further optimized. The wave propagators also provide the Sommerfeld forerunner in a straightforward manner. Note that all the results for the wave propagators, developed in this paper, can be applied to the plane wave case with simple modifications.

The Neumann to Dirichlet operator $\mathcal{K}$ and its inverse provide the exact absorbing boundary conditions for the wave propagation problem. Moreover, an alternative and more direct technique is employed to calculate the explicit form for these operators, see Appendix A.

Furthermore, the physical meaning of the wave splitting has been made clear by an investigation of the contribution from the split fields to the flow of energy.

Acknowledgment

The work reported in this paper is partially supported by a grant from the Swedish Research Council for Engineering Sciences and their support is gratefully acknowledged.

Appendix A Explicit forms for operators

The explicit form of the operators $\mathcal{K}$, $\mathcal{K}^{-1}$ and $\mathcal{K}^2$ in $(\boldsymbol{\rho}, n, \tau)$-space is derived in Ref. 47. Here, the sign of $\mathcal{K}$ is changed to be consistent with later work [20, 30, 49, 51]. In $(\boldsymbol{\lambda}, n, \tau)$-space the operators can be calculated directly by applying the two-dimensional Fourier transform. In $((\boldsymbol{r}, t))$-space the $\mathcal{K}$ operator is

$$\mathcal{K}v(\boldsymbol{\rho}, n, \tau) = \frac{1}{2\pi} \iint\limits_{U(\boldsymbol{\rho},\tau)} \frac{v(\boldsymbol{\rho}', n, \tau - R)}{R} d\boldsymbol{\rho}'.$$

Here $R = |\boldsymbol{\rho} - \boldsymbol{\rho}'|$ and $U(\boldsymbol{\rho}, \sigma)$ is a disc in the $\boldsymbol{\rho}'$-plane centered around $\boldsymbol{\rho}$ and with radius σ. A two-dimensional Fourier transform (3.1) and local polar coordinates

$\boldsymbol{\rho}' - \boldsymbol{\rho} = \boldsymbol{R}$ then lead to

$$\mathcal{K}v(\boldsymbol{\lambda}, n, \tau) = \int_0^\tau v(\boldsymbol{\lambda}, n, \tau - R) \frac{1}{2\pi} \int_0^{2\pi} e^{-i\lambda R \cos\alpha} d\alpha dR = \int_0^\tau v(\boldsymbol{\lambda}, n, \tau - R) J_0(\lambda R) dR.$$

where α is the angle between $\boldsymbol{\lambda}$ and $\boldsymbol{R}$. This implies that the kernel $K(\lambda, \tau) = H(\tau) J_0(\lambda\tau)$.

The Dirichlet to Neumann operator, see Ref. 47, can be represented as

$$\mathcal{K}^{-1} w = [\partial_\tau + \mathcal{L}] w,$$

where

$$\mathcal{L}w(\boldsymbol{\rho}, n, \tau) = -\frac{1}{2\pi} \iint_{U(\boldsymbol{\rho}, \tau)} \frac{\nabla' w(\boldsymbol{\rho}', n, \tau - R) \cdot (\boldsymbol{\rho}' - \boldsymbol{\rho})}{R^3} d\boldsymbol{\rho}'.$$

Using the above technique

$$\begin{aligned} \mathcal{L}w(\boldsymbol{\lambda}, n, \tau) =& -\frac{1}{2\pi} \iint_{\mathbb{R}^2} d\boldsymbol{\rho} \iint_{U(\boldsymbol{\rho}, \tau)} d\boldsymbol{\rho}' \frac{\nabla' w(\boldsymbol{\rho} + \boldsymbol{R}, n, \tau - R) \cdot \boldsymbol{R}}{R^3} e^{i\boldsymbol{\lambda} \cdot \boldsymbol{\rho}} \\ =& \int_0^\tau w(\boldsymbol{\lambda}, n, \tau - R) L(\lambda, R) dR. \end{aligned}$$

The kernel L is obtained by direct identification

$$L(\lambda, R) = -\frac{1}{R} \frac{d}{dR} \left(\frac{1}{2\pi} \int_0^{2\pi} e^{-i\lambda R \cos\alpha} d\alpha \right) = \lambda J_1(\lambda R)/R$$

For $\mathcal{K}^2$ Weston [47] derived

$$\mathcal{K}^2 v(\boldsymbol{\rho}, n, \tau) = \frac{1}{2\pi} \int_0^\tau ds \iint_{U(\boldsymbol{\rho}, \tau - s)} d\boldsymbol{\rho}' \frac{v(\boldsymbol{\rho}', n, s)}{[(\tau - s)^2 - R^2]^{1/2}}.$$

The application of the Fourier transformation and the introduction of the local polar coordinates then lead to

$$\begin{aligned} \mathcal{K}^2 v(\boldsymbol{\lambda}, n, \tau) =& \frac{1}{2\pi} \iint_{\mathbb{R}^2} d\boldsymbol{\rho} \int_0^\tau ds \iint_{U(\boldsymbol{\rho}, \tau - s)} d\boldsymbol{\rho}' \frac{v(\boldsymbol{\rho} + \boldsymbol{R}, s)}{[(\tau - s)^2 - R^2]^{1/2}} e^{i\boldsymbol{\lambda} \cdot \boldsymbol{\rho}} \\ =& \int_0^\tau v(\boldsymbol{\lambda}, n, s) M(\lambda, \tau - s) ds. \end{aligned}$$

As expected, cf. Ref. [20]

$$M(\lambda,\tau) = \frac{1}{2\pi}\int_0^\tau RdR\int_0^{2\pi} d\alpha \frac{e^{-i\lambda R\cos\alpha}}{[\tau^2-R^2]^{1/2}}$$
$$= \tau\int_0^1 sJ_0(\lambda\tau s)\frac{ds}{\sqrt{1-s^2}} = \frac{1}{\lambda}\sin(\lambda\tau),$$

where the last integral is given by Ref. 17, formula 6.554.2. From these results it is clear that the split fields in the present paper are the two-dimensional Fourier transforms of the physical split fields defined by Weston [47].

Appendix B Invariant imbedding and Green functions

To see the relation between the imbedding and Green functions formulations, use the representation, cf. (4.4)

$$\partial_\tau \mathbf{A}^{++}(n,\tau)* = \mathbf{A}^{++}(n,0^+) + \mathbf{A}_\tau^{++}(n,\tau)*\,.$$

The part of $\mathcal{P}^{++}$ corresponding to $\mathbf{A}^{++}(n,0^+)$ is then identified as the wave front propagator

$$\mathcal{Q}^+(n_2,n_1) = \mathbf{Q}^+(n_2,n_1) = \mathcal{S}\exp\left(\int_{n_1}^{n_2}\mathbf{A}^{++}(n,0^+)dn\right),$$

with

$$\mathbf{A}^{++}(n,0^+) = \mathbf{\Delta}_{11}(n,0^+).$$

Define propagators $\mathcal{T}^+$ and $\mathcal{G}^{++}$ which factor the propagator $\mathcal{P}^{++}(n_2,n_1)$ as

$$\mathcal{P}^{++}(n_2,n_1) = \mathcal{Q}^+(n_2,n_1)\mathcal{T}^+(n_2,n_1) = \mathcal{G}^{++}(n_2,n_1)\mathcal{Q}^+(n_2,n_1).$$

These factors have the explicit solutions, see (6.10)

$$\mathcal{T}^+(n_2,n_1) = \mathcal{S}\exp\left(\int_{n_1}^{n_2}\mathbf{Q}^+(n_1,n)\mathbf{A}_\tau^{++}(n,\tau)\mathbf{Q}^+(n,n_1)dn*\right),$$
$$\mathcal{G}^{++}(n_2,n_1) = \mathcal{S}\exp\left(\int_{n_1}^{n_2}\mathbf{Q}^+(n_2,n)\mathbf{A}_\tau^{++}(n,\tau)\mathbf{Q}^+(n,n_2)dn*\right).$$

By inspection, it is possible to represent the propagators $\mathcal{T}^+$ and $\mathcal{G}^{++}$ as integral operators with kernels $\mathbf{T}^+$ and $\mathbf{G}^{++}$ defined by

$$\mathcal{T}^+(n_2,n_1) = \mathbf{I}_\parallel + \mathbf{T}^+(n_2,n_1,\tau)*\,,$$
$$\mathcal{G}^{++}(n_2,n_1) = \mathbf{I}_\parallel + \mathbf{G}^{++}(n_2,n_1,\tau)*\,.$$

From the composition rules (6.2) it is then easy to see that $\mathbf{T}^{+}(n_1, n_2, \tau)$ is the resolvent to $\mathbf{G}^{++}(n_2, n_1, \tau)$ from the left, i.e.,

$$\mathbf{T}^{+}(n_1, n_2, \tau) + \mathbf{G}^{++}(n_2, n_1, \tau) + \mathbf{T}^{+}(n_1, n_2, \tau) * \mathbf{G}^{++}(n_2, n_1, \tau) = \mathbf{0}.$$

Moreover, these kernels are generalizations of the traditional transmission kernel and the corresponding Green function [4, 16, 29]. The imbedding and Green functions technique correspond to the fixed endpoints $n_2 = d$ and $n_1 = 0$, respectively, i.e., the propagator $\mathcal{T}^{+}(d, n)$ and $\mathcal{G}^{++}(n, 0)$.

Appendix C Domain for the Sommerfeld forerunner

The objective of this appendix is to investigate when the Sommerfeld forerunner is the dominant contribution to the early time behavior of the propagator. To do this, factor the propagator $\mathcal{P}^{++}$ using the decomposition $\mathcal{A}^{++}(n) = \mathcal{A}_{\mathrm{S}}^{++}(n) + \mathcal{A}_{\mathrm{rest}}^{++}(n)$ where

$$\begin{cases} \mathcal{A}_{\mathrm{S}}^{++}(n) = \mathbf{A}^{++}(n, 0^{+}) + \mathbf{A}_{\tau}^{++}(n, 0^{+}) * , \\ \mathcal{A}_{\mathrm{rest}}^{++} = \mathbf{Y}(n, \tau) * = [\mathbf{A}_{\tau}^{++}(n, \tau) - \mathbf{A}_{\tau}^{++}(n, 0^{+})] * . \end{cases}$$

Rewrite the propagator as a product, see Subsection 6.3, i.e.,

$$\mathcal{P}^{++}(n_2, n_1) = \mathcal{P}_{\mathrm{L}}^{++}(n_2, n_1)\mathcal{P}_{\mathrm{rest}}^{++}(n_2, n_1),$$

where

$$\begin{cases} \mathcal{P}_{\mathrm{rest}}^{++}(n_2, n_1) = \mathcal{S} \exp\left(\displaystyle\int_{n_1}^{n_2} \mathbf{Y}(n, \tau) dn * \right), \\ \mathcal{P}_{\mathrm{L}}^{++}(n_2, n_1) = \mathcal{S} \exp\left(\displaystyle\int_{n_1}^{n_2} \mathcal{P}_{\mathrm{rest}}^{++}(n_2, n)\mathcal{A}_{\mathrm{S}}^{++}(n)\mathcal{P}_{\mathrm{rest}}^{++}(n, n_2) dn \right). \end{cases}$$

In order to investigate the contribution from the last term, define the kernel $\mathbf{P}_{\mathrm{rest}}$ by

$$\mathcal{P}_{\mathrm{rest}}^{++} - \mathcal{I} = \mathbf{P}_{\mathrm{rest}}(n_2, n_1, \tau) * .$$

The kernels $\mathbf{P}_{\mathrm{rest}}$ and $\mathbf{Y}(n, \tau)$ satisfy the integral equation

$$\mathbf{P}_{\mathrm{rest}}(n_2, n_1, \tau) = \int_{n_1}^{n_2} \mathbf{Y}(n, \tau) dn + \int_{n_1}^{n_2} \mathbf{Y}(n, \tau) * \mathbf{P}_{\mathrm{rest}}(n, n_1, \tau) dn.$$

Define the iteration scheme, $k = 0, 1, 2, \ldots$

$$\mathbf{P}_{\mathrm{rest}}^{(k+1)}(n_2, n_1, \tau) = \int_{n_1}^{n_2} \mathbf{Y}(n, \tau) dn + \int_{n_1}^{n_2} \mathbf{Y}(n, \tau) * \mathbf{P}_{\mathrm{rest}}^{(k)}(n, n_1, \tau) dn$$

with initial value $\mathbf{P}_{\mathrm{rest}}^{(0)} \equiv \mathbf{0}$. The solution is then obtained as the series

$$\mathbf{P}_{\mathrm{rest}} = \sum_{k=0}^{\infty} \left(\mathbf{P}_{\mathrm{rest}}^{(k+1)} - \mathbf{P}_{\mathrm{rest}}^{(k)} \right),$$

provided the series converges. Define the norm

$$\|\mathbf{A}\| = \sup_{\substack{n\in[n_1,n_2]\\ \tau\in[0,T]}} \|\mathbf{A}(n,\tau)\|_D,$$

where $\|\cdot\|_D$ is any dyadic norm that satisfies the Schwartz inequality, i.e.,

$$\|\mathbf{A}\cdot\mathbf{B}\|_D \le \|\mathbf{A}\|_D\|\mathbf{B}\|_D.$$

The above series gives a unique solution for all bounded $\|\mathbf{Y}\|$, $|n_2-n_1|$, and T since, by induction, the following estimate holds [22]

$$\|\mathbf{P}^{(k+1)}_{\rm rest}(n_2,n_1,\tau) - \mathbf{P}^{(k)}_{\rm rest}(n_2,n_1,\tau)\|_D \le \frac{\|\mathbf{Y}\|^{k+1}|n_2-n_1|^{k+1}T^k}{k!(k+1)!}.$$

Thus

$$\|\mathbf{P}_{\rm rest}(n_2,n_1,\tau)\|_D \le \sqrt{\frac{\|\mathbf{Y}\||n_2-n_1|}{T}} I_1\left(2\sqrt{\|\mathbf{Y}\||n_2-n_1|T}\right).$$

Here, the modified Bessel function I_1 is used.

Recall the standard definition of operator norm

$$\|\mathcal{U}\| = \sup_{\boldsymbol{F}} \frac{\|\mathcal{U}\boldsymbol{F}\|}{\|\boldsymbol{F}\|}.$$

Using operator norm

$$\|\mathcal{P}^{++}_{\rm rest} - \mathcal{I}\| = T\|\mathbf{P}_{\rm rest}\|.$$

This result implies that the rest term can be neglected for $\|\mathbf{Y}\||n_2-n_1|T \ll 1$. Note that $\|\mathbf{Y}\|$ can be made arbitrarily small, if T is sufficiently small provided $\mathbf{A}^{++}_\tau(n,\tau)$ is right-continuous at $\tau=0$. Therefore, $|n_2-n_1|$ can be made large and simultaneously $\|\mathbf{Y}\|\,|n_2-n_1|$ is held constant.

The rule (6.10) implies that

$$\mathcal{P}^{++}_{\rm L} = \mathcal{S}\exp\left(\int_{n_1}^{n_2} \mathcal{P}^{++}_{\rm rest}(n_2,n)\mathcal{A}^{++}_{\rm S}(n)\mathcal{P}^{++}_{\rm rest}(n,n_2)dn\right)$$

which is close to the Sommerfeld propagator since $\mathcal{P}^{++}_{\rm rest} \approx \mathcal{I}$. Now, factor the Sommerfeld propagator (the propagator with $\mathcal{P}^{++}_{\rm rest} = \mathcal{I}$) as a product, i.e., $\mathcal{P}^{++}_S = \mathcal{Q}^+\mathcal{P}^{++}_{\rm R}$ where $\mathcal{Q}^+ = \mathbf{Q}^+\cdot$ is the wave front propagator, cf. Appendix B. Using the above technique it is straightforward to obtain

$$\|\mathcal{P}^{++}_{\rm R} - \mathcal{I}\| \le \sqrt{\xi} I_1\left(2\sqrt{\xi}\right),$$
$$\xi = \|\mathbf{Q}^+\|^2\|\mathbf{A}^{++}_\tau(n,0^+)\|\,|n_2-n_1|T.$$

From this expression, it is obvious that if the parameter ξ is small, then the Sommerfeld forerunner is close to the wave front propagator $\mathbf{Q}^+$, and no precursor effects are seen.

References

[1] I. Åberg, G. Kristensson, and D. J. N. Wall. Propagation of transient electromagnetic waves in time-varying media—direct and inverse scattering problems. *Inverse Problems*, **11**(1), 29–49, 1995.

[2] E. Ammicht, J. P. Corones, and R. J. Krueger. Direct and inverse scattering for viscoelastic media. *J. Acoust. Soc. Am.*, **81**, 827–834, 1987.

[3] L. M. Barkovskii, G. N. Borzdov, and A. V. Lavrinenko. Fresnel's reflection and transmission operators for stratified gyroanisotropic media. *J. Phys. A: Math. Gen.*, **20**, 1095–1106, 1987.

[4] R. S. Beezley and R. J. Krueger. An electromagnetic inverse problem for dispersive media. *J. Math. Phys.*, **26**(2), 317–325, 1985.

[5] J. D. Bjorken and S. D. Drell. *Relativistic Quantum Fields*. McGraw-Hill, New York, 1965.

[6] C. F. Bohren and D. R. Huffman. *Absorption and Scattering of Light by Small Particles*. John Wiley & Sons, New York, 1983.

[7] L. Brillouin. *Wave propagation and group velocity*. Academic Press, New York, 1960.

[8] J. P. Corones, M. E. Davison, and R. J. Krueger. Direct and inverse scattering in the time domain via invariant imbedding equations. *J. Acoust. Soc. Am.*, **74**(5), 1535–1541, 1983.

[9] J. P. Corones, M. E. Davison, and R. J. Krueger. The effects of dissipation in one-dimensional inverse problems. In A. J. Devaney, editor, *Inverse Optics, Proceedings of the SPIE*, pages 107–114, Bellingham, WA, 1983. Proc. SPIE 413, SPIE.

[10] J. P. Corones, G. Kristensson, P. Nelson, and D. L. Seth, editors. *Invariant Imbedding and Inverse Problems*. SIAM, Philadelphia, 1992.

[11] J. P. Corones and Z. Sun. Transient Reflection and Transmission Problems for Fluid-Saturated Porous Media. In J. P. Corones, G. Kristensson, P. Nelson, and D. L. Seth, editors, *Invariant Imbedding and Inverse Problems*. SIAM, 1992.

[12] J. P. Corones and Z. Sun. Simultaneous reconstruction of material and transient source parameters using the invariant imbedding method. *J. Math. Phys.*, **34**(5), 1824–1845, 1993.

[13] J. Fridén. Inverse scattering for anisotropic mirror image symmetric media. *Inverse Problems*, **10**(5), 1133–1144, 1994.

[14] J. Fridén. Relations between scattering data and material parameters in complex media. Technical Report LUTEDX/(TEAT-7038)/1–12/(1995), Lund Institute of Technology, Department of Electromagnetic Theory, P.O. Box 118, S-211 00 Lund, Sweden, 1995.

[15] J. Fridén. Inverse scattering for the homogeneous dispersive anisotropic slab using transient electromagnetic fields. *Wave Motion*, **23**(4), 289–306, 1996.

[16] J. Fridén, G. Kristensson, and R. D. Stewart. Transient electromagnetic wave propagation in anisotropic dispersive media. *J. Opt. Soc. Am. A*, **10**(12), 2618–2627, 1993.

[17] I. S. Gradshteyn and I. M. Ryzhik. *Table of Integrals, Series, and Products*. Academic Press, New York, fourth edition, 1965.

[18] S. He. A 'compact Green function' approach to the time domain direct and inverse problems for a stratified dissipative slab. *J. Math. Phys.*, **34**(10), 4628–4645, 1993.

[19] S. He. Frequency and time domain Green functions technique for nonuniform LCRG transmission lines with frequency-dependent parameters. *J. Electro. Waves Applic.*, **7**(1), 31–48, 1993.

[20] S. He and A. Karlsson. Time domain Green function technique for a point source over a dissipative stratified half-space. *Radio Sci.*, **28**(4), 513–526, 1993.

[21] S. He and S. Ström. The electromagnetic scattering problem in the time domain for a dissipative slab and a point source using invariant imbedding: Reconstrucion of the permittivity and conductivity. *J. Comp. Appl. Math.*, **42**, 137–155, 1992.

[22] E. Hille. *Methods in classical and functonal analysis*. Addison-Wesley, Reading, MA, USA, 1972.

[23] J. D. Jackson. *Classical Electrodynamics*. John Wiley & Sons, New York, second edition, 1975.

[24] A. Karlsson. Inverse scattering for viscoelastic media using transmission data. *Inverse Problems*, **3**, 691–709, 1987.

[25] A. Karlsson. Wave propagators for transient waves in one-dimensional media. Technical Report LUTEDX/(TEAT-7041)/1–26/(1995), Lund Institute of Technology, Department of Electromagnetic Theory, P.O. Box 118, S-211 00 Lund, Sweden, 1995.

[26] A. Karlsson and G. Kristensson. Constitutive relations, dissipation and reciprocity for the Maxwell equations in the time domain. *J. Electro. Waves Applic.*, **6**(5/6), 537–551, 1992.

[27] A. Karlsson and R. Stewart. Wave propagators for transient waves in periodic media. *J. Opt. Soc. Am. A*, **12**(7), 1513–1521, 1995.

[28] K. L. Kreider. A wave splitting approach to time dependent inverse scattering for the stratified cylinder. *SIAM J. Appl. Math.*, **49**, 932–943, 1989.

[29] G. Kristensson. Direct and inverse scattering problems in dispersive media—Green's functions and invariant imbedding techniques. In R. Kleinman, R. Kress, and E. Martensen, editors, *Direct and Inverse Boundary Value Problems*, Methoden und Verfahren der Mathematischen Physik, Band 37, pages 105–119, Frankfurt am Main, 1991. Peter Lang.

[30] G. Kristensson. Transient electromagnetic wave propagation in waveguides. *J. Electro. Waves Applic.*, **9**(5/6), 645–671, 1995.

[31] G. Kristensson and R. J. Krueger. Direct and inverse scattering in the time domain for a dissipative wave equation. Part 1: Scattering operators. *J. Math. Phys.*, **27**(6), 1667–1682, 1986.

[32] G. Kristensson and R. J. Krueger. Direct and inverse scattering in the time domain for a dissipative wave equation. Part 2: Simultaneous reconstruction of dissipation and phase velocity profiles. *J. Math. Phys.*, **27**(6), 1683–1693, 1986.

[33] G. Kristensson and R. J. Krueger. Direct and inverse scattering in the time domain for a dissipative wave equation. Part 3: Scattering operators in the presence of a phase velocity mismatch. *J. Math. Phys.*, **28**(2), 360–370, 1987.

[34] G. Kristensson and R. J. Krueger. Direct and inverse scattering in the time domain for a dissipative wave equation. Part 4: Use of phase velocity mismatches to simplify inversions. *Inverse Problems*, **5**(3), 375–388, 1989.

[35] G. Kristensson and S. Rikte. Scattering of transient electromagnetic waves in reciprocal bi-isotropic media. *J. Electro. Waves Applic.*, **6**(11), 1517–1535, 1992.

[36] G. Kristensson and S. Rikte. The inverse scattering problem for a homogeneous bi-isotropic slab using transient data. In L. Päivärinta and E. Somersalo, editors, *Inverse Problems in Mathematical Physics*, pages 112–125. Springer-Verlag, Berlin, 1993.

[37] G. Kristensson and S. Rikte. Transient wave propagation in reciprocal bi-isotropic media at oblique incidence. *J. Math. Phys.*, **34**(4), 1339–1359, 1993.

[38] I. V. Lindell, A. H. Sihvola, S. A. Tretyakov, and A. J. Viitanen. *Electromagnetic Waves in Chiral and Bi-isotropic Media*. Artech House, Boston, London, 1994.

[39] J. Lundstedt and S. Ström. Simultaneous reconstruction of two parameters from the transient response of a nonuniform LCRG transmission line. *J. Electro. Waves Applic.*, **10**(1), 19–50, 1996.

[40] T. H. O'Dell. *The Electrodynamics of Magneto-electric Media*. North-Holland, Amsterdam, 1970.

[41] H. Otterheim. *Time domain direct and inverse scattering for gyrotropic media*. PhD thesis, Royal institute of technology, Stockholm, Sweden, 1993.

[42] R. Redheffer. On the relation of transmission-line theory on scattering and transfer. *J. Math. Phys.*, **41**, 1–41, 1962.

[43] M. Reed and B. Simon. *Methods of modern mathematical physics*, volume II: Fourier analysis, Self-adjointness. Academic Press, New York, 1975.

[44] S. Rikte. *Propagation of transient electromagnetic waves in stratified bi-isotropic media and related inverse scattering problems*. PhD thesis, Lund Institute of Technology, Department of Electromagnetic Theory, P.O. Box 118, S-211 00 Lund, Sweden, 1994.

[45] S. Rikte. Sommerfeld's forerunner in stratified isotropic and bi-isotropic media. Technical Report LUTEDX/(TEAT-7036)/1–26/(1994), Lund Institute of Technology, Department of Electromagnetic Theory, P.O. Box 118, S-211 00 Lund, Sweden, 1994.

[46] R. D. Stewart. *Transient electromagnetic scattering on anisotropic media*. PhD thesis, Iowa State University, Ames, Iowa, 1989.

[47] V. H. Weston. Factorization of the wave equation in higher dimensions. *J. Math. Phys.*, **28**, 1061–1068, 1987.

[48] V. H. Weston. Wave splitting and the reflection operator for the wave equation in $\mathbb{R}^3$. *J. Math. Phys.*, **30**(11), 2545–2562, 1989.

[49] V. H. Weston. Invariant imbedding for the wave equation in three dimensions and the applications to the direct and inverse problems. *Inverse Problems*, **6**, 1075–1105, 1990.

[50] V. H. Weston. Invariant imbedding and wave splitting in $\mathbb{R}^3$: II. The Green function approach to inverse scattering. *Inverse Problems*, **8**, 919–947, 1992.

[51] V. H. Weston. Time-domain wave-splitting of Maxwell's equations. *J. Math. Phys.*, **34**(4), 1370–1392, 1993.